An Asynchronous Entanglement Distribution Protocol for Quantum Networks

Zhaoying Wang, Jian Li, Kaiping Xue, Shaoyin Cheng, Nenghai Yu, Qibin Sun, and Jun Lu

Abstract

Entanglement-based quantum networks can provide unconditionally secure communication by distributing entangled pairs between distant end nodes. To achieve end-to-end entanglement distribution, multiple operations of entanglement swapping in a quantum repeater chain are always required. However, due to the non-determinism of entanglement swapping caused by imperfect physical devices, the execution pattern of swapping operations has a direct impact on the performance of entanglement distribution, which can be categorized into an entanglement access control (EAC) problem. In this article, we attribute the EAC problem to two aspects: the matching optimization within quantum nodes, and the swapping conflict avoidance between quantum nodes. Accordingly, we propose an asynchronous entanglement distribution protocol which contains a custom weighted maximum matching algorithm, and a reliable signaling interaction mechanism to avoid a swapping conflict, respectively. Based on the proposed protocol, quantum repeaters autonomously decide their behaviors and spontaneously construct the end-to-end entangled pairs asynchronously. Simulation results show that our protocol can significantly improve the entanglement distribution rate and fidelity of end-to-end entangled pairs while simplifying the deployment and management process of the quantum networks.

Introduction

Quantum technology is poised to bring the next technological revolution. As a pivotal part of quantum technology, a quantum network is expected to be a promising platform that can support various cutting-edge quantum applications, including secure communication by teleportation [1], distributed quantum computing, and quantum sensing [2]. Most of these applications require sharing long-distance entangled pairs between end nodes. Hence, end-to-end entanglement distribution is the premise of the future quantum applications.

An EPR pair is a specific entangled state of two particles, which can be used as the most basic communication resources for entanglement-based quantum networks [3]. However, the success rate of entanglement distribution between two quantum nodes decays exponentially with the physical distance (e.g., in fiber), which makes physically transmitting entangled particles over long-distance inadvisable. Fortunately, entanglement swapping [4] can overcome the distance limitation by deploying several quantum repeaters between two end nodes. Specifically, end-to-end entanglement distribution can be achieved by performing Bell-state measurement (BSM) — a quantum operation with the aid of classical communication — at intermediate quantum repeaters [5]. However, due to the imperfection of quantum devices, BSM can only be performed with a certain success rate resulting in non-deterministic results of swapping. This non-determinism makes the end-to-end entanglement distribution unreliable and significantly reduces communication efficiency. Therefore, quantum repeaters have to make appropriate operational decisions based on the dynamically changing network status constantly. This decision realizes the entanglement access control (EAC), which reflects the subsequent behavior of an EPR pair, such as performing swapping, keeping stored, or being erased from storage.

The existing end-to-end entanglement distribution schemes can be divided into two categories: synchronous mode and asynchronous mode. Most studies are based on synchronous mode with centralized control, which collects network status (such as storage size and requests) within discrete time slots. Then the controller broadcasts the optimal decisions via the classic networks. For example, Shi et al. [6] proposed an entanglement routing algorithm based on synchronous time slots to build end-to-end paths for each request. However, centralized control brings additional computational overhead and higher latency (e.g., synchronization between repeaters), causing severe decoherence. Differently, to overcome the shortcoming of synchronous mode, Kozlowski et al. [7] presented a greedy asynchronous distribution protocol, in which all repeaters can perform swapping without order and aggregate the BSM results to end nodes. This protocol is designed to be efficient in the face of short quantum storage lifetimes. Nevertheless, greedy asynchronous swapping ignores the swapping failure detection, which will magnify the disadvantage of swapping (i.e., non-determinism) and reduce resource utilization because any single failed swapping will cause an invalid end-to-end entanglement distribution.

Basically, an efficient entanglement distribution needs to address the aforementioned challenges, that is, delay sensitivity and low resource

Digital Object Identifier:
10.1109/MNET.001.2200177

Zhaoying Wang, Jian Li (corresponding author), Kaiping Xue, Shaoyin Cheng, Nenghai Yu, Qibin Sun and Jun Lu are with the University of Science and Technology of China, China.

0890-8044/22/$25.00 © 2022 IEEE

utilization. Hence, in this article, we propose an improved asynchronous distribution protocol to achieve EAC without a centralized controller and to detect swapping failure much sooner through signaling interaction. The main contributions of our work are summarized as follows:

- We model the EAC as matching optimization within quantum nodes and swapping conflict avoidance between quantum nodes. Accordingly, we propose an asynchronous entanglement distribution protocol to tackle the EAC problem for the seek of efficient end-to-end entanglement distribution.
- Our proposed protocol involves a custom weighted maximum matching algorithm to optimize matching results within quantum nodes, and a signaling interaction mechanism and controlling the entangled particles by defining the storage unit's state to avoid swapping conflict.
- We implement the proposed asynchronous entanglement distribution protocol in our discrete event-driven quantum simulator, SimQN, and make an extensive performance evaluation. Based on the simulation results, the proposed protocol shows significant superiority over the current work in terms of final fidelity and entanglement distribution rate (EDR).

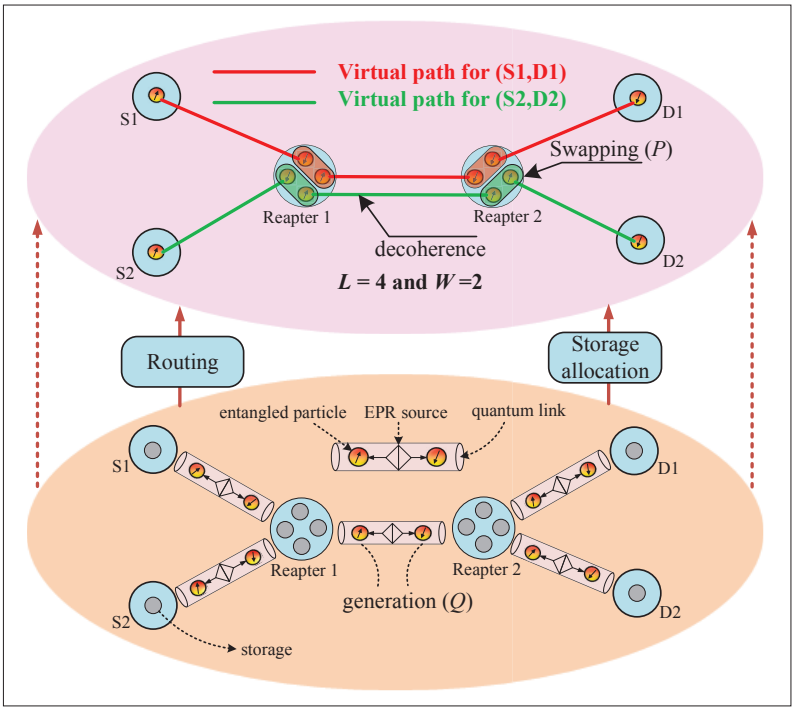

FIGURE 1. A typical example of an entanglement-based quantum network. Along the virtual path, end-to-end EPR pairs can be distributed by performing swapping at repeaters.

Background and Motivation

Generation, Swapping, and Fidelity

Link-layer entanglement generation and swapping are necessary operations to distribute end-to-end entangled pairs. Nevertheless, imperfect quantum devices cause uncertainty in quantum gate/measurement operations. Hence, entanglement generation and swapping are non-deterministic, whose success rate can be denoted as Q and P, respectively, as shown in Fig. 1. Meanwhile, the success of entanglement generation and swapping can be detected by quantum measurement, that is, the messages heralding the success or failure of the attempts can be traveled between nodes.

An EPR pair has limited lifetime and can become decoherent, as shown in Fig. 1. Typically, we use *fidelity* (a value between 0 and 1) to quantify the probability that an EPR pair can stay in the maximum entanglement state. For example, an invalid EPR pair implies that its *fidelity* is below 0.5. If a swapping fails or an EPR pair is kept in storage longer than "cutoff" time [8], the affected pair will be zeroed out and entanglement generation has to start over again.

Virtual Path Model

Our protocol is connection-oriented, which requires a so-called virtual path [9] to be established between one pair of end nodes for each request. Currently, there are various routing algorithms (implemented in a globally controlled [6, 10] or distributed network [11]) for entanglement-based quantum networks, which can be adopted to output an appropriate virtual path of fixed length L and link bandwidth W, as shown in Fig. 1. The length L indicates the number of nodes along this path. Link bandwidth W represents the number of storage units allocated for the request by each node on the virtual path. Conveniently, we can divide the allocated storage space of any repeater for each request into two parts (half of W) logically, which are used to share EPR pairs with its predecessor and successor, respectively. Each repeater knows the storage unit's index of each entangled particle and can perform BSM on two selected entangled particles. When entanglement swapping fails, quantum nodes have the ability to free the allocated storage units and store the regenerated EPR pairs.

In analogy to the classical networks, functional allocation in a quantum network protocol stack is proposed in [12–15]. When a static virtual path is determined, an EPR source existing on the link between any adjacent nodes runs entanglement generation protocol [12] in order to keep adjacent nodes being entangled. We assume that each link has a fixed maximum distribution rate of R, which means that R entanglement generation can be attempted per unit time. Repeaters will determine whether to receive the incoming entangled particles according to the current storage capacity. We design the upper layer entanglement distribution protocol based on this robust link entanglement generation.

Motivation

In the synchronous mode, there is a centralized controller to collect network status in each time slot to make optimal decisions. However, considering that the computational overhead and delay increases rapidly with the scale of the network, so scheme based on global network synchronization is not suitable which leads to severe quantum decoherence.

For asynchronous mode, each repeater in a virtual path is entirely independent to decide whether and when to perform an entanglement swapping operation. Entanglement swapping can

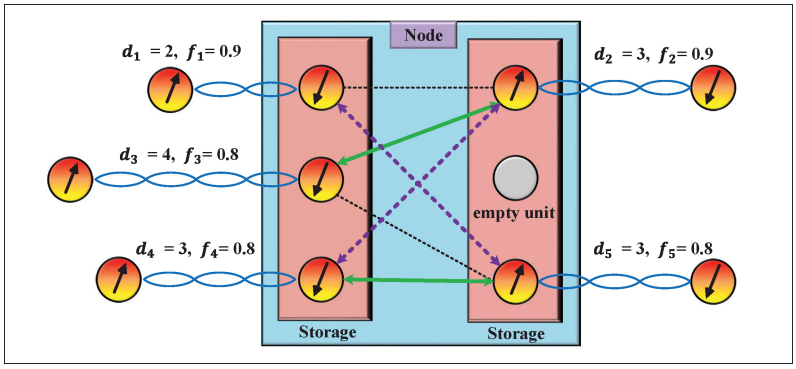

FIGURE 2. A typical matching optimization problem in a quantum node. The green solid line is the output of the maximum match. The purple dotted line represents a common match.

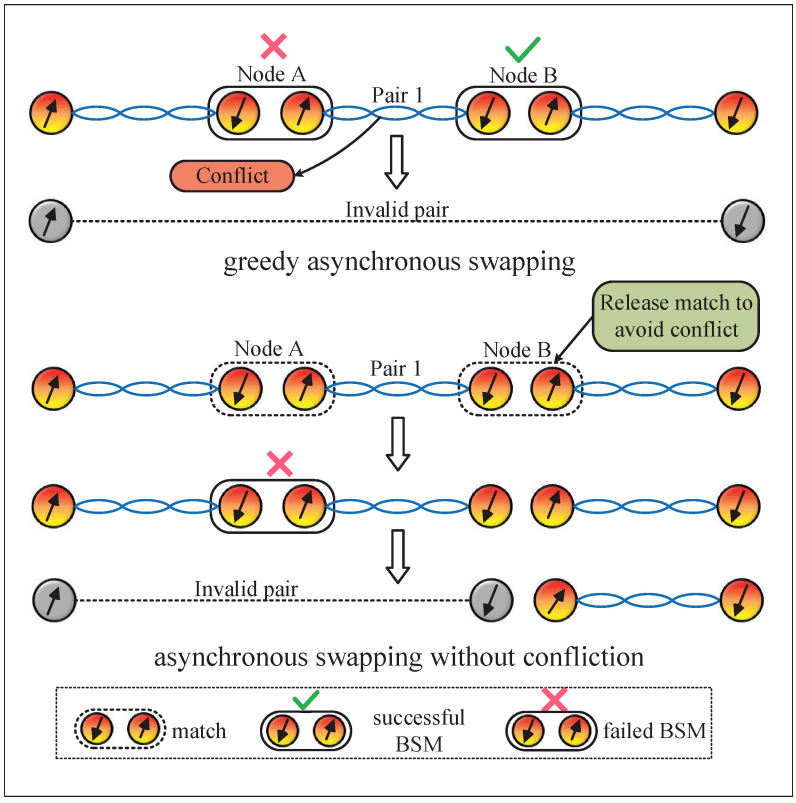

FIGURE 3. Greedy asynchronous swapping with conflict and our improved asynchronous swapping without conflict.

be executed as soon as two EPR pairs entangled with predecessor and successor in the same virtual path are available. However, representative work [7] (greedy asynchronous swapping) lacks timely failure detection in the swapping process. No error detection will result in the undesirable situation that any failed swapping operation at a repeater would affect the end-to-end entanglement distribution. In order to overcome such defects, we should timely detect swapping errors in the entanglement distribution process to achieve efficient resource utilization. The key is to implement access control to entanglement resources within and between nodes.

Entanglement Access Control (EAC)

The access to the EPR pairs must be carefully coordinated among the entangled nodes. Any uncoordinated action from one of the entangled nodes would result in the irreversible destruction of the entanglement resource. For our improved end-to-end entanglement distribution, the access to the EPR pairs mainly involves two aspects, namely selecting two entangled particles to perform BSM and avoiding resource sharing caused by the situation where both two nodes attempt to apply BSM to the same EPR pair simultaneously. Hence, we can generalize EAC as two aspects: matching optimization in nodes and swapping conflict avoidance between nodes.

In-Node: Matching Optimization

There may be several EPR pairs in the two storage spaces of each repeater. These EPR pairs may originate from the primary link (between adjacent nodes) or may be shared by two nodes spanning multiple nodes. In order to distribute a longer-distance EPR pair, each node should pick two entangled particles from two separate storage spaces, and then perform BSM on the extracted entangled particles to complete the swapping operation. Since there could be multiple entangled particles in one quantum storage, there will be a matching optimization problem to determine which two entangled particles should be jointly measured, as shown in Fig. 2. An optimal matching algorithm can reduce the waiting time of EPR pairs in storage.

Between Nodes: Swapping Conflict Avoidance

If one EPR pair is measured by two adjacent nodes simultaneously, this situation can be named as swapping conflict. An example is given on top of Fig. 3. For the existing greedy swapping scheme, swapping conflict (e.g., pair 1 involves two BSMs in Node A and Node B) exists on the virtual path. The failure of the BSM at any repeater along the path will destroy the end-to-end entanglement distribution, even if the BSMs on other repeaters are successful. The core reason for this drawback is that conflicts between nodes hinder to detect failed swapping in time.

Each repeater should track the swapping result in time to avoid swapping conflict. As shown at the bottom of Fig. 3, if swapping conflict occurs, one of the two BSMs should be released. In other words, if BSM is performed on one particle of one EPR pair, another particle of this pair must be restricted from measurement until this swapping is completed. By comparison, if we avoid conflicts between adjacent nodes, the damage caused by a single-repeater BSM failure is limited, and we only regenerate EPR pair on the related links instead of the entire path.

Protocol Design and Implementation

Weighted Maximum Matching

Analogous to the Maximum-Weight bipartite matching problem in a weighted bipartite graph, a quantum repeater can utilize the *Hungarian* algorithm[1] to calculate the optimal matching results. All entangled particles in the two-part storage can construct a fully weighted bipartite graph, as shown in Fig. 2. Now, what we need to address is the definition of the weight for each match.

[1] The Hungarian algorithm is a combinatorial optimization algorithm for solving task assignment problems in polynomial time. Therefore, the computation cost of the maximum matching is negligible compared to the propagation delay of the signals.

Any repeater can collect the following information: the entanglement distance (d) between the particles of each EPR pair shared by this repeater (which can be considered as the number of hops), and the current *fidelity* (f) which represents the entanglement quality. We consider the decoherence model which involves the following two aspects: entanglement swapping and decoherence caused by long-term storage. Entanglement swapping will cause a simple product form $f_{swap} = f_1 \times f_2$, where f_1, f_2 represents the fidelity of two EPR pairs performing swapping. Long-term storage can also cause a drop in entanglement quality. The current fidelity f_c which can be calculated by the difference between the its birth time T_b and the current time T_c (exponential decay with time $e^{-k\cdot\Delta t}$, $\Delta t = T_c - T_b$, k varies in different storage medium). So, $f_c = f_b \times e^{-k\cdot\Delta t}$, where f_b represents the fidelity at birth time. We can calculate the fidelity of each EPR pair at any time based on these two models. Each repeater can use these local information to design function $V = C(f_1, d_1, f_2, d_2)$. $f_{1(2)}$, $d_{1(2)}$ means the current fidelity and distance of each EPR pair, respectively. We can utilize $C(.)$ to output a computable real number V as the weight for each match.

A new EPR pair created by entanglement swapping has an additive distance and an approximate product fidelity. Therefore, we design a comprehensive weight

$$V = w_1 \cdot (d_1 + d_2) + w_2 \cdot (f_1 \cdot f_2),\ w_1 \geq w_2.$$

The reasons are as follows. Longer-distance entanglement is formed by more entanglement swappings certainly, so it is more precious and is preferentially matched for the next entanglement swapping. When the entanglement distance is the same, the EPR pair with higher fidelity has a longer survival time and is more conducive to end-to-end entanglement distribution. In conclusion, entanglement distance dominates the matching results and the fidelity plays an auxiliary role. Since d is expressed in terms of hops (an integer at least 1), f does not exceed 1, entanglement distance dominates the matching results when the $w_1 \geq w_2$ condition is satisfied, which is consistent with our design goals. For example, we can set $w_1 = 1$, $w_2 = 1$.

As shown in Fig. 2, we get two possible matching results: Maximum match (green solid line):

$$V_{max} = [w_1 \cdot (d_2 + d_3) + w_2 \cdot (f_2 \cdot f_3)] + [w_1 \cdot (d_4 + d_5) + w_2 \cdot (f_4 \cdot f_5)] = 14.36.$$

Common match (purple dotted line):

$$V_{com} = [w_1 \cdot (d_1 + d_5) + w_2 \cdot (f_1 \cdot f_5)] + [w_1 \cdot (d_2 + d_4) + w_2 \cdot (f_2 \cdot f_4)] = 12.44.$$

Obviously, $V_{max} > V_{com}$. This node chooses a better maximum match represented by the green solid line by comparing the V. In this way, the node preferentially matches longer-distance and higher-fidelity EPR pair combinations, which meets our expectations.

Storage Unit's State Control

In order to realize the access control of entangled particles by multiple operations of different nodes, each node should set and maintain a "state" for each entangled particle on a logical level. Moreover, this state is not instantaneous and often needs to be maintained for a period of time to ensure the independent access of entangled particles between different operations. For convenience, we can realize the access control of entangled particles by checking the state of the corresponding storage units. We define three storage unit's states (*Free*, *Matching*, *Occupied*) and describe the default behavior restrictions respectively, as shown in Fig. 4.

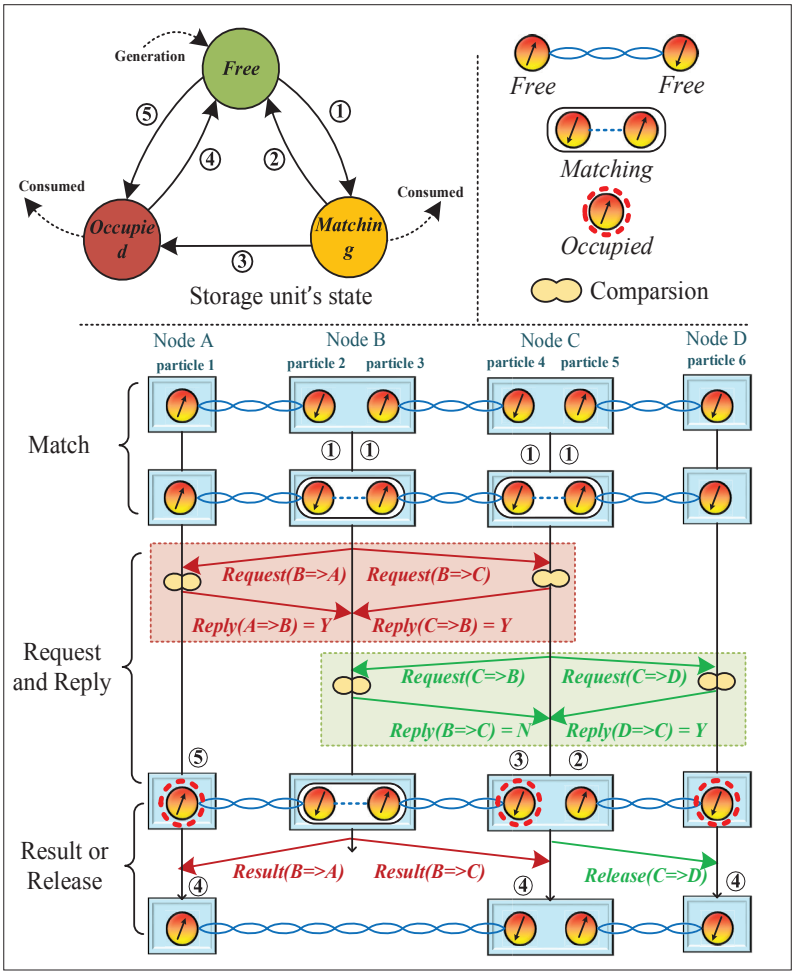

FIGURE 4. Storage unit's state and transformation between states. Example of protocol processing on a 4-node virtual path.

Free: When a new EPR pair is generated, or a longer EPR pair is created after entanglement swapping, each particle of this EPR pair needs to be set to *Free*. *Free* means that this particle is unconstrained and can be further matched with another particle. One particle will remain in *Free* if failing to match with other particles.

Matching: Repeaters can complete several matches between entangled particles spontaneously. When a match is determined, two entangled particles of this match will be transformed into *Matching* state to avoid simultaneous access to them by other operations. Before the match is released, the corresponding particle is locked. Besides, two entangled particles will not be measured directly after they transform into the Matching state because further interaction is required to avoid swapping conflict. If the match eventually

Signaling	Composition	Main function
Request	*Request* = {*src*, *dest*, *storage_index*, *V*}	Each spontaneously formed match issues a request to its entangled neighbors, aiming to achieve control over the corresponding entanglement resource. *V* is the weight calculation result for this match.
Reply	*Reply* = {*src*, *dest*, *storage_index*, *Y/N*}	Each node replies to the received request according to the local matching result by comparing *V*. *Y* represents that the node abandons the local matching attempt, and *N* represents that the node still retains control over the shared resources.
Result	*Result* = {*src*, *dest*, *storage_index*, *result/fail*}	A node decides to perform an entanglement swapping and sends the measurement results to both end nodes.
Release	*Release* = {*src*, *dest*, *storage_index*, *release*}	A node has been unable to receive *Y* replies from both sides, and has occupied the EPR pair for a long time without performing the swapping. Releasing corresponding resources avoids the waste.

TABLE 1. Compositions and main functions of signaling.

results in a BSM on those particles, the particle in *Matching* will be consumed.

Occupied: To resolve swapping conflict, two entangled particles of one EPR pair should not be measured at the same time. If one particle is used to perform BSM and then erased, another particle ought to construct a longer EPR pair. Therefore, the latter particle should be in *Occupied* to ensure the independence of this swapping within the time delay of transmission for measurement information. Particles in this state may also be consumed when failed swapping happens, which means that the particles used to restore the entanglement at both ends to be erased.

Signaling and Protocol

Signaling interaction is necessary to avoid the swapping conflict between nodes during end-to-end entanglement distribution. We need to define diverse signaling to meet different control requirements. In our protocol, four classic signalings: *Request*, *Reply*, *Result*, and *Release* are designed necessarily. We assume that the transmission of these classical packages is implemented by classical communication on the Internet. Furthermore, the classical networks can also be assumed to guarantee reliability, that is, determined transmission, but requires a certain delay. These necessary delays are often ignored in other solutions. Emphatically, the state of the entangled particle is not fixed and will change when signaling is received. Therefore, the condition of transformation between states also needs to be considered.

Request: All repeaters can run the maximum matching algorithm spontaneously and intermittently. There will be inevitable conflict when two nodes which attempt to measure an EPR pair at the same time, for instance the EPR pair between Node B and C in Fig. 4. Therefore, when a match is formed in a node, these two particles need to be set as *Matching* from *Free* until receiving other control signaling, as ① in Node B or C in Fig. 4. This node needs to make a *Request* containing the following information to predecessor and successor nodes to avoid such conflict, as *Request*(*B* ⇒ *A*) and *Request*(*B* ⇒ *C*). *Request* = {*src*, *dest*, *storage_index*, *V*}, where *src* and *dest* refer to the signaling sending node and receiving node, respectively. *storage_index* means the storage location of this EPR pair. *V* is the custom weight of this match. We can compare different matches based on this value.

Reply: When a node receives a *Request* from other nodes, this node needs to make a *Reply* to determine the availability of this *Request* by comparing the *V* of the requested match and local match (if it exists). If the local match is better, *Reply* is *N* (e.g., *Reply*(B ⇒ *C*)). Otherwise, *Reply* is *Y* (e.g., *Reply*(*C* ⇒ *B*)). Perhaps, the local entangled particle may not form a match which is in *Free*, thereby *Reply* is *Y* (e.g., *Reply*(*A* ⇒ *B*)) with changing state to *Occupied*, as ⑤ in Node A in Fig. 4. The signaling should contain the following: *Reply* = {*src*, *dest*, *storage_index*, *Y/N*}.

Any node may receive three bidirectional Reply combinations from its predecessor and successor. We can abbreviate them as *own*, *pre*, and *suc*. Next, we describe the default actions of *own* in each case in turn. It should be emphasized that receiving only one *Reply* from *pre* or *suc* is not enough to determine the following action, so the *own* needs to keep waiting for another *Reply*.

{*Reply*(*pre* ⇒ *own*) = *Y*, *Reply*(*suc* ⇒ *own*) = *Y*}: If the *Reply* in both directions (*pre* ⇒ *own* and *suc* ⇒ *own*) is *Y*, which means that the local match in *own* is the best between *own*, *pre*, and *suc*. Hence BSM can then be performed on *own* to form a longer EPR pair, as Node B in Fig. 4. The states of two particles in this local match will still be *Matching* before they are measured.

{*Reply*(*pre* ⇒ *own*) = *Y*, *Reply*(*suc* ⇒ *own*) = *N*}: In this case, the match at *suc* is the best, followed by *own* and *pre*, as Node C in Fig. 4. The match at *own* needs to be released. The particle entangled with *pre* should be set to *Free* and another particle entangled with *suc* should be set to *Occupied* because BSM may happen at *suc*, corresponding to ② and ③ in Node C in Fig. 4, respectively.

{*Reply*(*pre* ⇒ *own*) = *N*, *Reply*(*suc* ⇒ *own*) = *N*}: If the *Reply* in both directions (*pre* ⇒ *own* and *suc* ⇒ *own*) is *N*, which means that the local match is the worst between *own*, *pre*, and *suc*. The match in *own* must be released. A possible swapping will occur at either *pre* or *suc*. Thus, all the particles in this match should be set to *Occupied*.

Result/Release: The signaling here may include two options, depending on different *Reply* combinations as mentioned above. For example, when the *Reply*s in both directions are *Y*, *own* can perform BSM locally. If BSM is successful, *own* must distribute the measurement results to both *pre* (e.g., *Result*(*B* ⇒ *A*)) and *suc* (e.g., *Result*(*B* ⇒ *C*)). Accordingly, a new EPR pair is created while particle 1 and 4 become *Free* again, as ④ in Node A and C. Conversely, the associated quantum storage units of *own*, *pre* and suc need to be erased for regeneration when BSM fails, so *Result* = {*src*, *dest*, *storage_ index*, *result/fail*}.

If the two *Reply*s in the two directions are dif-

ferent, let us assume that the matches are sorted as follows: *suc* > *own* > *pre*. The match at *own* needs to be released. However, at this time, the corresponding particle on *pre* still considers that the swapping may occur at *own*, which causes a long-time deadlock error. Therefore, *own* needs to inform *pre* to stop waiting through a *Release* package. Thus, the state of corresponding particle on *pre* can be transfered into *Free* from *Occupied*, corresponding to ④ in Node D and *Release*($C \Rightarrow D$) in Fig. 4. We can design *Release* = {*src*, *dest*, *storage_index*, *release*}.

Finally, the composition and main function about signaling is shown below to make the difference between signaling more apparent as shown in Table 1.

Simulation

We use SimQN (https://github.com/ertuil/SimQN), which is a discrete-event-based network simulation platform for quantum networks to support our simulation. We present two performance metrics: entanglement distribution rates (*EDR*) and final fidelity. *EDR* means the average number of available end-to-end EPR pairs per second. Final fidelity means the average fidelity of all distributed end-to-end EPR pairs. We compare the performance differences caused by different matching mechanisms in our scheme. Then we compare with the greedy asynchronous swapping scheme about their EDR.

We list the parameters of the simulation as follows. The path length L increases from 4 nodes to 12 nodes. The success rate of entanglement generation is Q = 0.8. The success rate of swapping is P = 0.6. The entanglement generation rate R = 50 times per second. The fidelity of the initially generated EPR pairs is random in the range (0.9, 0.99). Each repeater includes W = 100 storage units. The transmission delay of classic packets is 0.02 seconds. We set decoherence coefficient k = 0.01, 0.1, and 0.3. The matching weight is set to w_1 = 1, w_2 = 1.

Comparison of Different Matching Mechanisms

We set the decoherence coefficient k = 0.3. We compare maximum matching (MM) with random matching (RM) about their performance difference on EDR and final fidelity. Random matching means that any repeater select particles in *Free* to form a match randomly without considering *d* and *f*. Additionally, we define the increased rate (η) to visually reflect the difference in performance. For example, increased rate of *EDR* can be calculated as: $(EDR_{MM} - EDR_{RM})/EDR_{RM}$. Increased rate of final fidelity is $[(F_{MM} - 0.5) - (F_{RM} - 0.5)]/(F_{RM} - 0.5) = (F_{MM} - F_{RM})/(F_{RM} - 0.5)$.

As shown in Fig. 5a and b, in general, our designed maximum matching algorithm represents higher-EDR and higher-fidelity end-to-end EPR pairs. Primarily, it is to be expected that the η of EDR will be more significant when L becomes larger (when L = 11, 12, the maximum matching has almost doubled the improvement of EDR of random matching). This result is attributed to the maximum matching algorithm by utilizing more information (*d* and *f*) to make matching decisions. More precious long-distance and high-fidelity EPR pairs will be preferentially matched to perform entanglement swapping, which shortens the

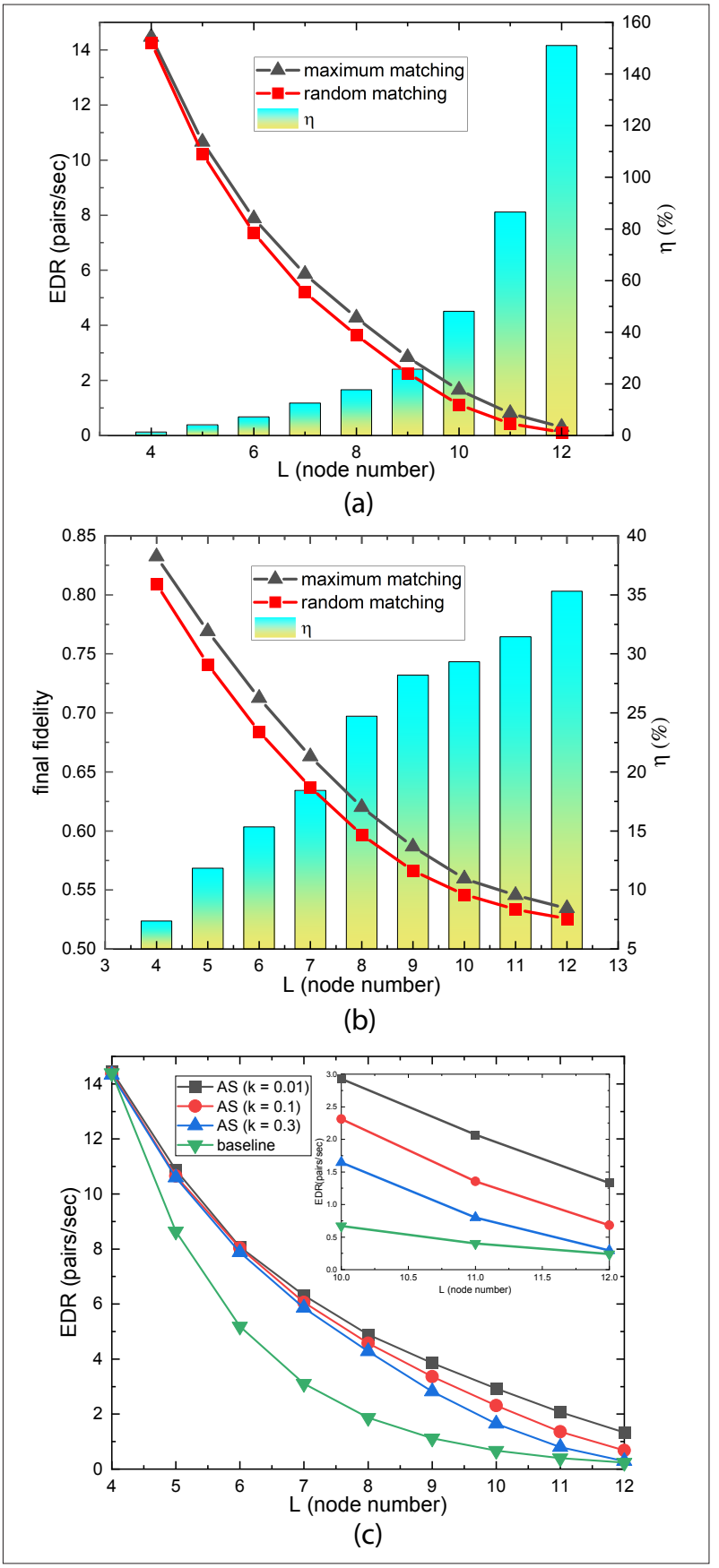

FIGURE 5. Analysis of simulation results: a) EDR of maximum matching and random matching; b) Final fidelity of maximum matching and random matching; c) EDR of greedy asynchronous swapping (baseline) and our improved asynchronous swapping (AS) with decoherence coefficient k = 0.01, 0.1, and 0.3.

More precious long-distance and high-fidelity EPR pairs will be preferentially matched to perform entanglement swapping, which shortens the delay of end-to-end entanglement distribution. Therefore, the *EDR* can be increased and the final fidelity can be less attenuated by reducing the negative impact of decoherence.

delay of end-to-end entanglement distribution. Therefore, the *EDR* can be increased and the final fidelity can be less attenuated by reducing the negative impact of decoherence.

Comparison of Different Protocols

For our scheme, we consider three settings, k = 0.01, 0.1, and 0.3, respectively. To get a theoretical upper bound on EDR of baseline, we ignore the transmission delay of classical information, consider that the storage is unlimited, and ignore the negative impact of fidelity attenuation, which is a very loose setting. L – 2 entanglement swappings are required to distribute end-to-end EPR pairs along a path with L nodes. Therefore, the probability of successfully creating an end-to-end entanglement is P^{L-2}. Therefore, the expectation of end-to-end EDR can be expressed as $EDR = R \times Q \times P^{L-2}$.

As shown in Fig. 5c, our scheme has a higher EDR (multiple advantages) than the greedy asynchronous swapping, reflecting the higher resource utilization brought by early failure detection. In addition, higher decoherence coefficients will lead to more severe decoherence, resulting in the descending *EDR* as k increases. Moreover, the differences in *EDR* due to different decoherence coefficients (k) will become more apparent as the number of nodes increases. Because the time overhead for interaction is low when there are fewer nodes, the impact of decoherence is minimal. When the number of nodes increases, the storage waiting time will increase with the more frequent interactions. The fidelity will decay exponentially with time, so the difference in *EDR* will be more obvious.

Conclusion

In this article, comparing with the centrally controlled scheme with a time-synchronous model or the greedy asynchronous distribution scheme, we designed an improved asynchronous entanglement distribution protocol. Our scheme addresses the problem of excessive latency and low resource utilization in the above existing solutions. Through simulations in SimQN, we verified the superiority of our protocol in EDR and fidelity compared with greedy asynchronous swapping. Therefore, on the premise of guaranteeing the performance of entanglement distribution, asynchronism makes our scheme easy to deploy and implement, which has a great significance for the future quantum network. Finally, purification can further enhance the quality assurance of end-to-end EPR pairs. We may consider a fusion approach that considers purification operations in our proposed asynchronous distribution protocol in future research.

Acknowledgment

This work is supported in part by Anhui Initiative in Quantum Information Technologies under grant No. AHY150300 and Youth Innovation Promotion Association Chinese Academy of Sciences (CAS) under Grant No. Y202093.

References

[1] D. Bouwmeester *et al.*, "Experimental Quantum Teleportation," *Nature*, vol. 390, no. 6660, 1997, pp. 575–79.
[2] W. Kozlowski and S. Wehner, "Towards Large-Scale Quantum Networks," *Proc. Sixth Annual ACM Int'l. Conf. Nanoscale Computing and Commun.*, 2019, pp. 1–7.
[3] B. F. Toner and D. Bacon, "Communication Cost of Simulating Bell Correlations," *Physical Review Letters*, vol. 91, no. 18, 2003, p. 187,904.
[4] H.-J. Briegel *et al.*, "Quantum Repeaters: The Role of Imperfect Local Operations in Quantum Communication," *Physical Review Letters*, vol. 81, no. 26, 1998, p. 5932.
[5] R. Van Meter and J. Touch, "Designing Quantum Repeater Networks," *IEEE Commun. Mag.*, vol. 51, no. 8, 2013, pp. 64–71.
[6] S. Shi and C. Qian, "Concurrent Entanglement Routing for Quantum Networks: Model and Designs," *Proc. Annual Conf. ACM Special Interest Group on Data Communication on the Applications, Technologies, Architectures, and Protocols for Computer Commun.*, 2020, pp. 62–75.
[7] W. Kozlowski, A. Dahlberg, and S. Wehner, "Designing a Quantum Network Protocol," *Proc. 16th Int'l. Conf. Emerging Networking Experiments and Technologies*, 2020, pp. 1–16.
[8] E. Shchukin, F. Schmidt, and P. van Loock, "Waiting time in Quantum Repeaters With Probabilistic Entanglement Swapping," *Physical Review A*, vol. 100, no. 3, 2019, p. 032,322.
[9] R. Van Meter *et al.*, "Path Selection for Quantum Repeater Networks," *Networking Science*, vol. 3, no. 1, 2013, pp. 82–95.
[10] Y. Zhao and C. Qiao, "Redundant Entanglement Provisioning and Selection for Throughput Maximization in Quantum Networks," *Proc. IEEE INFOCOM 2021–IEEE Conf. Computer Commun.*, IEEE, 2021, pp. 1–10.
[11] K. Chakraborty *et al.*, "Distributed Routing in a Quantum Internet," arXiv preprint arXiv:1907.11630, 2019.
[12] A. Dahlberg *et al.*, "A Link Layer Protocol for Quantum Networks," *Proc. ACM Special Interest Group on Data Commun.*, 2019, pp. 159–73.
[13] A. Pirker and W. Dür, "A Quantum Network Stack and Protocols for Reliable Entanglement-Based Networks," *New J. Physics*, vol. 21, no. 3, 2019, p. 033003.
[14] N. Yu, C.-Y. Lai, and L. Zhou, "Protocols for Packet Quantum Network Intercommunication," *IEEE Trans. Quantum Engineering*, vol. 2, 2021, pp. 1–9.
[15] Z. Li *et al.*, "Building a Large-Scale and Wide-Area Quantum Internet Based on an OSI-Alike Model," *China Commun.*, vol. 18, no. 10, 2021, pp. 1–14.

Biographies

Zhaoying Wang (wzy0716@mail.ustc.edu.cn) received his bachelor's degree from the School of Cyber Science and Technology, University of Science and Technology of China (USTC), in 2018. He is currently working toward the Ph.D. degree from the School of Cyber Science and Technology, USTC. His research interests include quantum networking and network security.

Jian Li [M'20] (lijian9@ustc.edu.cn) received his bachelor's degree from the Department of Electronics and Information Engineering, Anhui University, in 2015, and received his Ph.D. degree from the Department of Electronic Engineering and Information Science (EEIS), University of Science and Technology of China (USTC), in 2020. He is currently a Post-Doctoral fellow with the School of Cyber Science and Technology, USTC. His research interests include future Internet architecture design, satellite-terrestrial integrated networks, and quantum networking.

Kaiping Xue [M'09, SM'15] (kpxue@ustc.edu.cn) received his bachelor's degree from the Department of Information Security, University of Science and Technology of China (USTC), in 2003, and received his Ph.D. degree from the Department of Electronic Engineering and Information Science (EEIS), USTC, in 2007. Currently, he is a Professor in the School of Cyber Science and Technology, USTC. His research interests include future Internet architecture design, transmission optimization, network security, and quantum networking. He is a Fellow of the IET.

Shaoyin Cheng [M'20] (sycheng@ustc.edu.cn) received his bachelor's degree from the Department of Information Security, University of Science and Technology of China (USTC), in 2003, and received his Ph.D. degree from the Department of Computer Science and Technology, USTC, in 2009. He is currently a lecturer with the School of Cyber Science and Technology, USTC. His research interests include software security, protocol testing, and cyber security evaluation.

NENGHAI YU (ynh@ustc.edu.cn) received his bachelor's degree from Nanjing University of Posts and Telecommunications, Nanjing, China, in 1987, an M.E. degree from Tsinghua University, Beijing, China, in 1992, and his Ph.D. degree from the Department of Electronic Engineering and Information Science (EEIS), University of Science and Technology of China (USTC), Hefei, China, in 2004. Currently, he is a professor in the School of Cyber Science and Technology, USTC. He is the executive dean of the School of Cyber Science and Technology, USTC, and the director of the Information Processing Center, USTC. His research interests include multimedia security and quantum networking.

QIBIN SUN [F'11] (qibinsun@ustc.edu.cn) received a Ph.D. degree from the Department of Electronic Engineering and Information Science (EEIS), University of Science and Technology of China (USTC), in 1997. He is currently a professor in the School of Cyber Science and Technology, USTC. His research interests include multimedia security, network intelligence and security, and so on. He has published more than 120 papers in international journals and conferences.

JUN LU (lujun2019@ustc.edu.cn) received his bachelor's degree from Southeast University in 1985 and his master's degree from the Department of Electronic Engineering and Information Science (EEIS), University of Science and Technology of China (USTC), in 1988. He is currently a professor in the School of Cyber Security and Technology and the Department of EEIS, USTC. His research interests include theoretical research and system development in the field of integrated electronic information systems. He is an Academician of the Chinese Academy of Engineering (CAE).